Correlation-Based Template Tracking Of Moving Object

Original Scientific Paper

Hema Tekwani
Harcourt Butler Technical University,
Research Scholar, Department of Electronics Engineering
Kanpur, India
hematekwani19@gmail.com

Krishna Raj
Harcourt Butler Technical University,
Professor and Head, Department of Electronics Engineering
Kanpur, India
kraj_biet@yahoo.com

Abstract *– This paper presents the correlation-based motion estimation technique for the 3D displacement of objects. Two high-speed cameras are configured as a stereovision system and synchronized in real-time. Finger and hand motions are captured in form of digital images at 1500 fps and 2000 fps respectively. A complete motion acquisition system is calibrated to determine the intrinsic and extrinsic parameters which were later used in the correlation algorithm. The grayscale image frames acquired from the cameras are correlated using square templates of 10x10 pixels created from the reference image. The finger and hand motion are discussed with varying camera speed as a measure of brightness inconsistency. The observations in the correlation coefficient indicate that the proposed algorithm is efficient up to 20 and 50 templates for the finger and hand motion cases respectively. The correlation coefficient for finger motion was increased to 0.987 and 0.972 for the left and right cameras, respectively, while the correlation coefficient for hand motion was 0.924 and 0.898. The proposed algorithm is developed in MATLAB and validated by tracing the sinusoidal motion of a solid rectangular element from the image correlation technique and an accelerometer sensor mounted over the block.*

Keywords*: Grayscale Speckling, Motion Estimation, Stereo-Rig, Template, Template Tracking Coefficient, Thresholding*

1. INTRODUCTION

Flow-based motion estimation is a well-established method for tracking moving object features. The explicit application of flow-based methods in feature matching makes real-time motion estimation difficult. Since image information does not vary significantly from frame to frame, real-time motion analysis is critical in image processing. This further becomes extremely interesting to find the trajectory of moving objects with small displacements without altering the image quality. To find the best match frame, a full search technique [1] is employed in which sub-bands are used to separate the images according to their spatial and temporal orientation [2], [3]. Flow-based feature tracking has received a lot of attention, and feature-based approaches have become popular for describing distinctive visual features [4]. Computations for local motions are done in the vector field, where a motion patch [5] represents the motion, various feature attributes were included in previous motion assessment studies. The motion-tracking algorithm is developed and modified with spatial and temporal information to restore any missing feature point in tracking [6]. Another advancement was alignment in the image to find the corresponding coordinate set in the warped image [7]. To minimize intensity variations, the Lucas-Kanade algorithm also computes spatio-temporal derivatives. [8]. Researchers have attempted to measure the dynamic displacement of objects, but variations in shade and light intensity made it difficult to obtain precise results [9]. Additional algorithms are utilized in the feature tracking process, such as the warp update rule [10] in video coding motion. The illumination and lens distortion factors are also included in the iterative and hierarchical motion estimation algorithms [11]. To reduce complexity in multi-view video coding, motion and disparity estimation algorithms are used, resulting in a reduction in coding performance [12]. To retain image quality, the high-efficiency video coding standard has recently been used [13]. In another motion estimation study, Horn and Schunck developed a variational framework

that included data integrity and data matching [14]. Block matching algorithm is generally used but the hardware cost in high definition full search algorithm is a major concern [15]. Lee *et al*. implemented the searching and matching phase [16] in motion estimation by reducing the sum of absolute difference in the fast matching approach. Shen *et al*. [17] proposed the mode complexity and motion homogeneity to reduce the computational difficulty in motion and disparity estimation in multi-view coding. Most of the motion-tracking algorithms include features obtained from digital images. The digital image correlation algorithm includes subset-based correlation and element-based global correlation [18]. It was found that most of the optical flow estimation methods assume the constant brightness intensity of a pixel under the frame-wise displacement. Another approach that uses the optical flow-based framework is the gradient-based image correlation [19]. The motion estimation algorithm should be capable of countering the brightness effect and correlating the image features simultaneously with pixel-level accuracy [20]. The emergence of image correlation lies in the correlation of frames using a subset produced from a reference image [21]. The image correlation algorithm that approximates the internal and external parameters requires camera calibration [22]. Multiple square templates are obtained from the region of interest in a reference image. Monin et al. [23] modified the single-pixel algorithm and studied it with moving object frames for piece-wise 2D linear motion in single-pixel imaging. The root mean square error estimated with no regularization was 0.22. The investigation, however, was limited to simply planar motion. When using a non-cyclic basis, the technique results in a high level of reconstruction complexity. When the background is static, the local motion algorithm is limited. The root mean square error calculated in this work is 0.18 [24], and it describes a high-resolution motion measuring approach. In the present study, we propose a correlation-based three-dimensional motion estimation algorithm, which works on matching the grayscale intensity of a pattern, also called a template. Images of the moving object are captured using two high-speed cameras. The lens [25] correction in the form of both radial and tangential distortions, are calculated during camera calibration and are mentioned in the calibration Table in Section (3). The camera system is first calibrated [26] using MATLAB camera calibration application. The sets of image frames are correlated using templates to obtain template tracking coefficient or correlation coefficient (CC). We developed template-making and correlation algorithms in MATLAB. Three motion cases are investigated with the algorithm including finger and hand motion. The effect of the number of templates and speckle size on the CC is studied.

2. PROPOSED CORRELATION ALGORITHM

The templates are coupled in a correlation algorithm to estimate pixel displacement in 2D or 3D space. Generally, two cameras are preferred to estimate the three-dimensional location of the templates [27] [28].

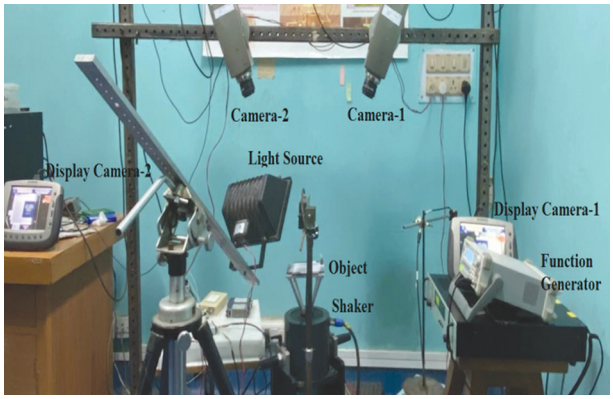

Fig. 1. Experimental Setup

The 3D motion estimation [29] demands that the object should remain in focus during the motion and the region of interest on the object is imaged on two or more cameras [19]. Since the motion of the object also depends on the camera speed, if the motion is slow then it should be correlated at a lower speed. A sufficient camera speed is able to obtain micron level displacement and time resolution. The thresholding [24] of the template and the formation of the subset also play a vital role in estimating the motion traversed. Fig. 1 shows the experimental setup and Fig. 2 shows the proposed image correlation algorithm. The algorithm involves the stereo camera calibration, image correlation, and validation of the correlation algorithm using an accelerometer sensor.

2.1. TEMPLATE TRACKING IN MOTION ESTIMATION

The template [30], [31] is correlated to a sequence of images to produce the pixel displacement. The technique is extremely helpful when motion features of the object under deliberation are not accessible. For tracking the grayscale intensity values, image correlation is performed and CCs are studied. Sutton *et al.* [27] described the CC for m observations of variables *a* and *b* as given in Equation (1). Where *a*' and *b*' are the mean values of a and b. For a perfect template matching in subsequent images, the CCs are unity [24].

$$Cor(a,b) = \frac{\sum_{j=1}^{m}(a_j - a')(b_j - b')}{\sqrt{\sum_{j=1}^{m}(a_j - a')^2 \sum_{j=1}^{m}(b_j - b')^2}} \quad (1)$$

The geometrical model for a camera requires three elementary transformations. The first transformation relates the world coordinates of a scene point to camera coordinates. The second transformation is the projection of this point onto the retinal plane. The third transforms the point into the sensor coordinate system [27]. Assuming a point in 3D space with its coordinates (X_w, Y_w, Z_w) where *w* signifies the world coordinate system and the camera [18] coordinates (*X, Y, Z*). The sen-

sor coordinates are (x_p, y_p) the focal length coordinates in pixels are (f_x, f_y) and the center of the image plane [27] is (C_x, C_y). The final customized form of the equation including all the transformations and constraints is given in Equation (2).

$$\begin{bmatrix} X \\ Y \\ Z \end{bmatrix} = \begin{bmatrix} R_{11}R_{12}R_{13} \\ R_{21}R_{22}R_{23} \\ R_{31}R_{32}R_{33} \end{bmatrix} \begin{bmatrix} X_w \\ Y_w \\ Z_w \end{bmatrix} + \begin{bmatrix} T_x \\ T_y \\ T_z \end{bmatrix} \quad (2)$$

Where $[R]$ and $[T]$ are the components of rotation matrix and translation vector. The transformed and modified form of displacement in sensor coordinates is shown in Equation (3).

$$\begin{pmatrix} x_p \\ y_p \end{pmatrix} = \begin{pmatrix} C_x + f_x \frac{R_{11}X_w + R_{12}Y_w + R_{13}Z_w + T_x}{R_{31}X_w + R_{32}Y_w + R_{33}Z_w + T_z} \\ C_y + f_y \frac{R_{21}X_w + R_{22}Y_w + R_{23}Z_w + T_y}{R_{31}X_w + R_{32}Y_w + R_{33}Z_w + T_z} \end{pmatrix} \quad (3)$$

$$\begin{pmatrix} x_p \\ y_p \end{pmatrix} = \begin{pmatrix} C_x^j + f_x^j \frac{R_{11}^j X_w + R_{12}^j Y_w + R_{13}^j Z_w + T_x^j}{R_{31}^j X_w + R_{32}^j Y_w + R_{33}^j Z_w + T_z^j} \\ C_y^j + f_y^j \frac{R_{21}^j X_w + R_{22}^j Y_w + R_{23}^j Z_w + T_y^j}{R_{31}^j X_w + R_{32}^j Y_w + R_{33}^j Z_w + T_z^j} \end{pmatrix} \quad (4)$$

Two camera system [32] is employed for out-of-plane measurement of displacement as shown in Equation (4), where j ϵ N, (N = 1, 2). The parameter which describes the field of view is stereo-angle. The left camera is chosen as the reference camera and the parameters are calculated with respect to the reference camera. Lens distortion was included also in the calibration process giving rise to radial and tangential distortion. Tangential distortion is negligible as compared to the radial, hence ignored. Typically two coefficients are sufficient for radial distortion [27].

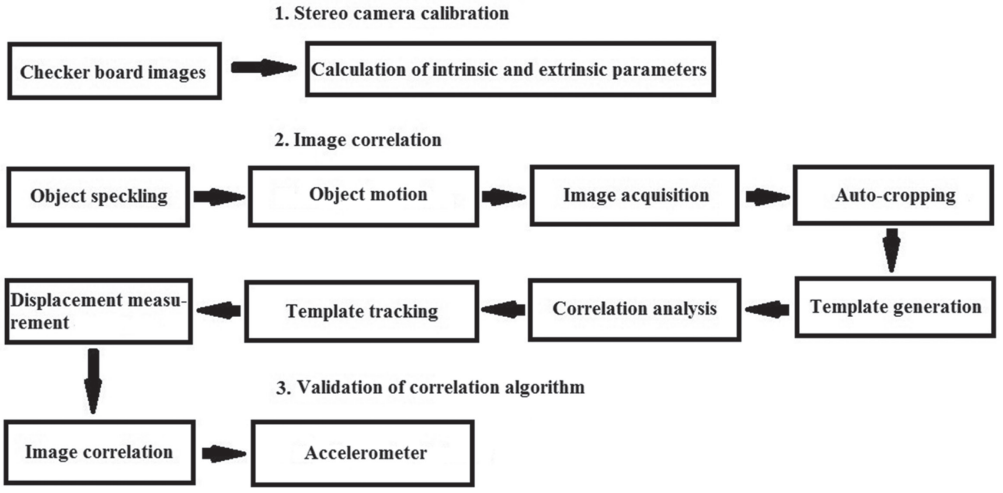

Fig. 2. Image Correlation Algorithm

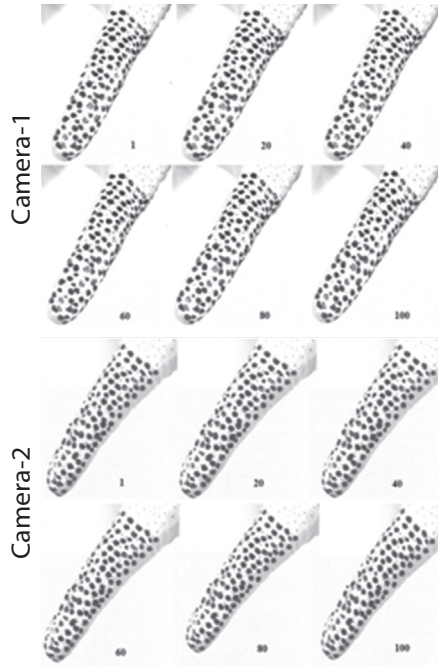

Fig. 3. Image frames for Finger Motion from Camera-1 and Camera-2

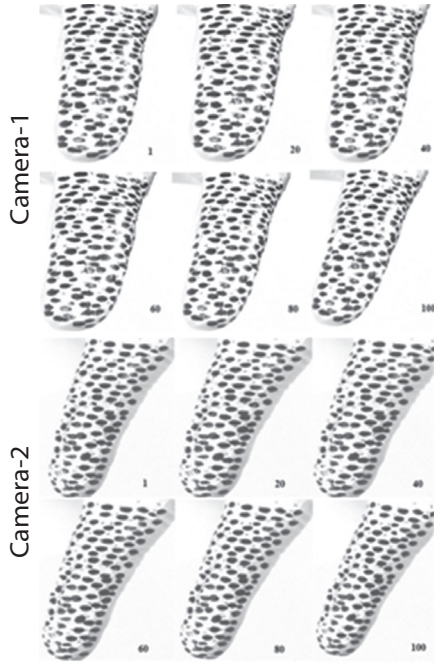

Fig. 4. Image frames for Finger Motion after Rotation from Camera-1 and Camera-2

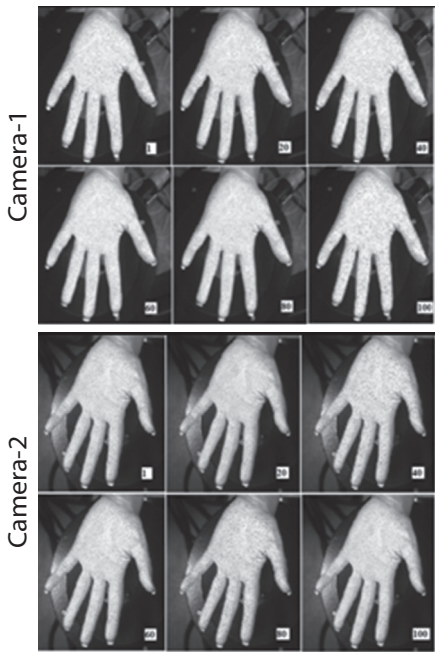

Fig. 5. Image frames for Hand Motion from Camera-1 and Camera-2

2.2. OBJECT SPECKLING AND TEMPLATE GENERATION

The algorithm follows the subset produced from a reference image in subsequent grayscale images. For the image correlation algorithm, objects are speckled in grayscale. Templates are developed from the first image of the reference camera. All images obtained from the left and right cameras, or camera-1 and camera-2, are correlated using the generated templates.

2.3. CORRELATION

The focus is adjusted by camera lenses, while the constant camera speed is essential for proper lighting. The Light should be sufficient for the templates to be visible and clear. The burst of 100 frames is captured and correlation is performed in all the frames as mentioned in Section 2.1. The CC is calculated as a measure of how efficiently the algorithm is implemented in images for template-based feature tracking.

3. EXPERIMENTAL

3.1. CALIBRATION

The 3D world coordinates (X_w, Y_w, Z_w) and the coordinates of the camera (X, Y, Z), need to be perfectly aligned. The grid also known as checker-board is used in calibration to calculate the intrinsic parameters e.g. focal length, principal point, distortion, and extrinsic parameters e.g. rotation and translation. A monochrome camera is preferred for perfect correlation. Two synchronized i-speed TR cameras (10000 FPS) and resolution (1280 x 1024 square pixels) with Nikon 50mm, 1:1.4D lenses are used in image correlation and for calibration and correlation. The lighting required in the process should be uniform and of adequate intensity, for the subset to correlate. Table (1), (2), and (3) shows the calibration data for finger motion, and Table (4), (5), and (6) shows the calibration for hand motion. The camera speed is selected based on the best object focus achieved in cameras [30]. The stereo camera calibration app in MATLAB is used for calibration. The checkerboard was placed in the field of view of cameras. Burst frame was set to unity and calibration grid was given small translation and rotation in random direction and images are acquired in both cameras using a common trigger. The angle between cameras was set to 34.5° at 1500fps and 42.6° at 2000fps. The angles were verified from extrinsic camera calibration parameters.

Table 1. Camera Calibration for 1500fps

Axis	Cam	Focal Length	Principal point
X	C1	2876.539 ± 15.705	666.061 ± 2.331
	C2	2151.659 ± 20.427	589.091 ± 2.017
Y	C1	3108.329 ± 16.365	623.902 ± 2.653
	C2	3095.646 ± 20.629	619.756 ± 2.169

Table 2. Distortion Parameters for 1500 fps

Axis	Cam	Radial	Tangential
X	C1	2.475 ± 0.139	0.001 ± 0.000
	C2	3.766 ± 0.206	0.004 ± 0.001
Y	C1	-433.388 ± 32.269	-0.007 ± 0.001
	C2	-903.849 ± 64.362	0.035 ± 0.001
Z	C1	23838.387 ± 2177.570	-
	C2	67071.699 ± 5985.477	-

Table 3. Position and Orientation of Camera-2 Relative to Camera-1 at 1500 fps

Axis	Rotation	Translation
X	-0.007 ± 0.001	-791.821 ± 3.883
Y	0.601 ± 0.002	5.363 ± 0.585
Z	-0.019 ± 0.001	345.907 ± 12.434

Table 4. Camera Calibration for 2000 fps

Axis	Cam	Focal Length	Principal point
X	C1	2883.706 ± 19.595	610.486 ± 7.263
	C2	2846.721 ± 32.167	586.3763 ± 17.936
Y	C1	2899.606 ± 20.078	565.609 ± 2.475
	C2	2788.549 ± 27.192	531.337 ± 6.315

Table 5. Distortion Parameters for 2000 fps

Axis	Cam	Radial	Tangential
X	C1	-1.748 ± 0.084	0.003 ± 0.001
	C2	0.556 ± 0.041	-0.007 ± 0.002
Y	C1	85.953 ± 9.265	-0.024 ± 0.002
	C2	-5.204 ± 1.036	-0.096 ± 0.004
Z	C1	-1648.520 ± 278.072	-
	C2	62.249 ± 14.187	-

3.2 OBJECT MOTION

Case-1: The motion of the finger in X, Y, and Z direction is captured, and required displacement in X_w, Y_w, and in Z_w is identified. Fig. 3 shows the image frames captured from both the cameras. It is found that the subsets formed in the process also capture the region that is not in the area of motion. Finger and hand motion were acquired in the 15th and 20th of a second respectively by adjusting camera speed. The short exposure time while capturing was chosen to acquire micro-scale motion in terms of 3D displacements.

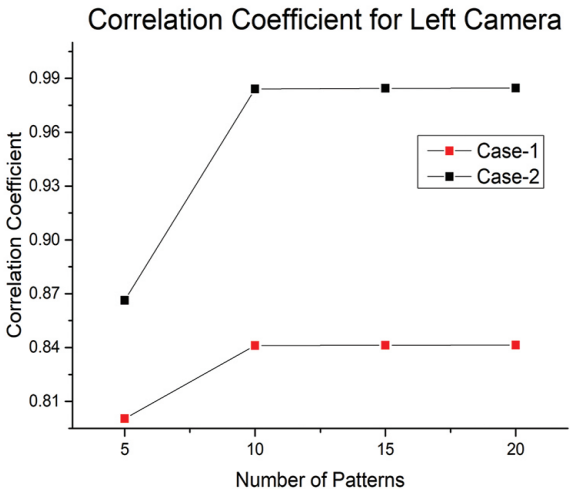

Fig. 6(a). Correlation Coefficient for Finger Motion from Camera-1

Table 7(a). Minimum Displacement for Finger Motion

Cases	Template	Minimum Displacement		
		X_w	Y_w	Z_w
Case-1	5	-127.810	-12.821	-1.092x10³
	10	-127.810	-12.821	-1.148x10³
	15	-142.345	-16.121	-1.189x10³
	20	-142.734	-16.607	-1.199x10³
Case-2	5	-101.921	-41.240	-1.209x10³
	10	-104.822	-59.539	-1.209x10³
	15	-138.121	-59.539	-1.216x10³
	20	-138.850	-59.651	-1.258x10³

Table 6. Position and Orientation of Camera-2 Relative to Camera-1 at 2000 fps

Axis	Rotation	Translation
X	-0.035 ± 0.002	-807.622 ± 8.697
Y	0.744 ± 0.006	-4.752 ± 1.142
Z	0.021 ± 0.001	273.609 ± 19.859

Hence for Case-2: rotation code is developed, by which excess area can be cropped easily. Fig. 4 shows the image frames after applying the rotation code. Case-3: Motion of a human hand is captured using the templates to further validate the proposed algorithm irrespective of object shape and movement. The hand is randomly translated in 3D space and motion is captured. The number of templates is increased to 50. Fig. 5 shows the image sets for hand motion. It was found that CC is almost similar for 15 and 20 templates as shown in Table 9.

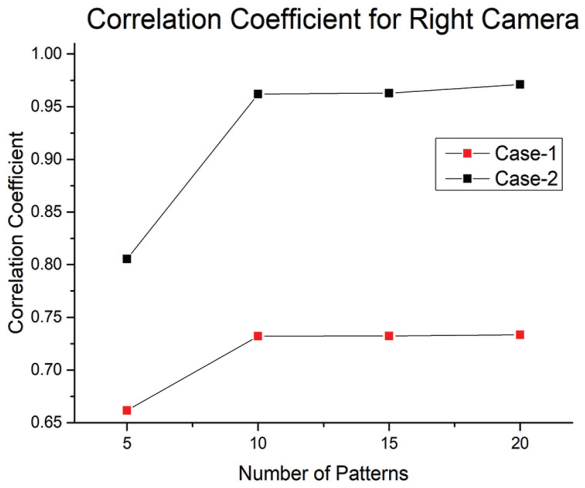

Fig. 6(b). Correlation Coefficient for Finger Motion from Camera-2

Table 7(b). Maximum Displacement for Finger Motion

Cases	Template	Maximum Displacement		
		X_w	Y_w	Z_w
Case-1	5	-38.129	258.973	-0.883x10³
	10	-38.129	258.973	-0.871x10³
	15	-42.333	268.923	-0.879x10³
	20	-42.793	269.134	-0.881x10³
Case-2	5	33.137	199.691	-0.845x10³
	10	33.137	201.359	-0.866x10³
	15	38.149	282.564	-0.889x10³
	20	38.154	282.987	-0.919x10³

The increment in CC with respect to the template size is attributed to the efficient matching of templates in the sequence images. To further propose the technique for large object motion estimation, a hand motion is captured and motion traversed in X, Y, and Z direction is calculated using 5, 10, 20, 30, 40, and 50 templates.

4. RESULTS AND DISCUSSION

4.1 MOTION MEASUREMENT

The correlation was performed for a fixed subset size of 10 and a threshold value >10. Tables 7 and 8 show displacement data for finger and hand motion up to 20 and 50 templates respectively. Six images are represented in Fig. 3, 4, and 5 out of 100 captured images for finger and hand motion considered.

4.2 EFFECT OF NUMBER OF TEMPLATES ON TEMPLATE TRACKING

Case-1 represents finger motion and the minimum and maximum displacement measurements are shown in Table 7(a) and 7(b). The finger image frames are rotated in Case-2 to eliminate excess area out of the region of interest. We observed a significant difference in CC. The increment in CC for left camera in case-2 is 8.2% for 5 templates, 17.0% for 10 templates, 17.2% for 15 templates and 20 templates. Similarly for right camera increment in CC is 21.6% for 5 templates, 31.3% for 10 templates, 31.5% for 15 templates and 32.4% for 20 templates. Fig. 6(a) and 6(b) show CC with the number of templates for Case-1 and Case-2 respectively.

Table 8(a). Minimum Displacement for Hand Motion

Case	Template	Minimum Displacement		
		X_w	Y_w	Z_w
Case-3	5	-266.769	99.169	-1.289x10³
	10	-209.746	207.174	-1.251x10³
	20	-301.008	144.432	-1.286x10³
	30	-335.446	-169.568	-1.277x10³
	40	-349.846	-239.659	-1.260x10³
	50	-349.979	-239.948	-1.255x10³

Table 8(b). Maximum Displacement for Hand Motion

Case	Template	Maximum Displacement		
		X_w	Y_w	Z_w
Case-3	5	-108.059	218.922	-1.228x10³
	10	-146.302	270.258	-1.256x10³
	20	-110.669	270.258	-1.226x10³
	30	-72.183	233.611	-1.222x10³
	40	-49.156	252.978	-1.266x10³
	50	-49.251	252.989	-1.269x10³

As shown in Tables 8 and 10, the displacement values and CC values for 40 and 50 templates are almost similar. We observed that the template number plays an important role in motion assessment, which is expressed in Table 10. The CC increases on increasing the number of templates and saturates at the value of 40 and further found similar for 40 and 50 templates. Fig 7(a) and 7(b) show the CC for hand motion.

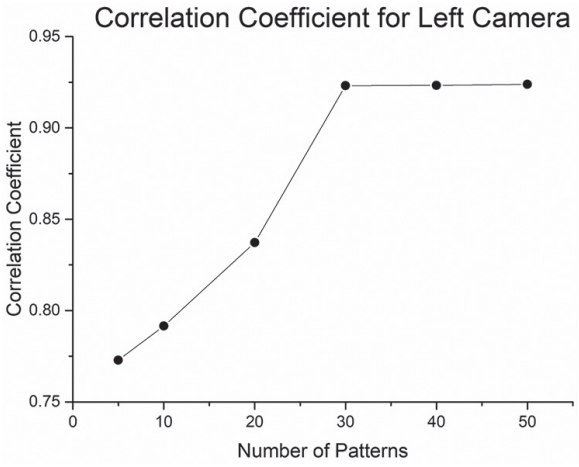

Fig. 7(a). Correlation Coefficient for Hand Motion from Camera-1

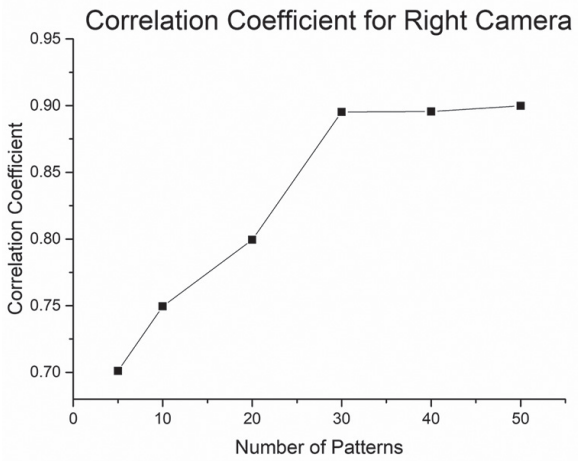

Fig. 7(b). Correlation Coefficient for Hand Motion from Camera-2

Template tracking is used to identify the location of templates with identical areas and different grayscale intensities. The area is in pixel units. The identical size templates were developed using a separate template-making algorithm. The correlation algorithm produces a match of a particular template only when it identifies the exact location of the template in the camera images.

Table 9. Correlation Coefficient for Finger Motion

Cases	Template	Correlation Coefficient	
		(Left Camera)	(Right Camera)
Case-1	5	0.801	0.662
	10	0.840	0.732
	15	0.841	0.733
	20	0.842	0.734
Case-2	5	0.867	0.805
	10	0.983	0.961
	15	0.986	0.964
	20	0.987	0.972

Table 10. Correlation Coefficient for Hand Motion

Cases	Template	Correlation Coefficient (Left Camera)	Correlation Coefficient (Right Camera)
Case-3	5	0.774	0.702
	10	0.793	0.751
	20	0.838	0.799
	30	0.921	0.895
	40	0.923	0.896
	50	0.924	0.898

4.3. VALIDATION OF THE ALGORITHM

The proposed technique was validated on a rigid aluminum block fixed using a fixture to the shaker. Half of the block was speckled using black and white paint whereas an accelerometer was mounted on the other half. A known frequency of 10 Hz was given through a function generator and a power amplifier. The motion of the block was captured using the same high-speed cameras and an image correlation algorithm was applied. The displacement response from both accelerometer and image correlation technique were compared. Fig. 8 shows the validation of the correlation algorithm.

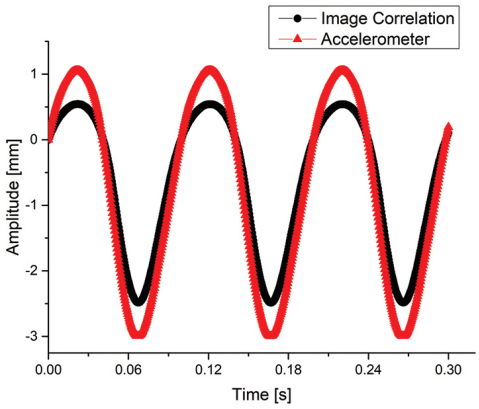

Fig. 8. Validation of Correlation Algorithm

5. CONCLUSION

The present study aimed to estimate object motion using the non-contact image correlation method. High-speed cameras are used in correlating the templates generated from the reference image to the images acquired from both cameras. Camera calibration is done before correlation to calculate the intrinsic and extrinsic parameters. The displacement was calculated using an image correlation technique in three cases: finger motion, rotating finger motion, and hand motion. Two high-speed cameras were synchronized in stereovision configuration to obtain CC. Case-1 and Case-2 represent finger motion with a constant shutter speed of 1500 fps. CC was found to increase up to 0.842 and 0.734 for cameras 1 and 2 respectively. For Case-2, an increase in CC goes up to 0.987 and 0.972 for cameras 1 and 2 respectively. The hand motion was studied at 2000 fps to further propose the algorithm for large objects motion measurement, CC was found to increase up to 0.924 and 0.898 for cameras 1 and 2 respectively, which is almost equivalent to that obtained in case-2. It was concluded that the proposed image correlation algorithm can be applied for motion estimation irrespective of speckle size for a constant template size. The CC was found to increase with the increase in template number.

6. ACKNOWLEDGEMENT

The authors would like to express their sincere gratitude to the Structures Lab at IIT Kanpur, where the experiments were carried out.

7. REFERENCES

[1] K. Singh, R. S. Ahamed, "Computationally efficient motion estimation algorithm for HEVC", Journal of Signal Processing Systems, 2017.

[2] Z. Wang, A. C. Bovik, A. R. Sheikh, E. P. Simoncelli, "Image quality assessment: from error visibility to structural similarity", IEEE Transactions on Image Processing, Vol. 13, No. 4, 2004, pp. 1-14.

[3] H. Tekwani, K. Raj, "Compression using thresholding on signal/image by applying wavelet analysis", Proceedings of the IEEE International Conference on Computational and Characterization Techniques in Engineering and Sciences, Lucknow, India, 14-15 September 2018, pp. 17-20.

[4] E. Antonakos, J. Alabort-i-Medina, G. Tzimiropoulos, S. P. Zafeiriou, "Feature-based Lucas-Kanade and active appearance models", IEEE Transactions on Image Processing, 2015, pp. 1-16.

[5] Y. Kellar, A. Averbuch, "Global parametric image alignment via high-order approximation", Computer Vision and Image Understanding, Vol. 109, 2008, pp. 244-259.

[6] J. Shin, S. Kim, S. Kang, S. W. Lee, J. Paik, B. Abidi, M. Abidi, "Optical flow-based real-time object tracking using non-prior training active feature model", Real-Time Imaging, Vol. 11, 2005, pp. 204-218.

[7] G. D. Evangelidis, E. Z. Psarakis, "Parametric image alignment using enhanced correlation coefficient maximization", IEEE Transactions on Pattern Analysis and Machine Intelligence, Vol. 30, No. 10, 2008, pp. 1-8.

[8] V. Mahalingam, k. Bhattacharya, N. Ranganathan, H. Chakravarthula, R. R. Murphy, K. S. Pratt, "A VLSI architecture and algorithm for Lucas-Kanade-based optical flow computation", IEEE Transactions on Very Large Scale Integration Systems, Vol. 18, No. 1, 2010, pp. 29-38.

[9] J. Guo, C. Zhu, "Dynamic displacement measurement of large-scale structures based on the Lucas-Kanade template tracking algorithm", Mechanical Systems and Signal Processing, Vol. 66-67, 2016, pp. 425-436.

[10] S. Baker, I. Matthews, "Lucas-Kanade 20 years on: a unifying framework", International Journal of Computer Vision, Vol. 53, No. 3, 2004, pp. 221-255.

[11] Y. Altunbasak, R. M. Mersereau, A. J. Patti, "A fast parametric motion estimation algorithm with illumination and lens distortion correction", IEEE Transactions on Image Processing, Vol. 12, No. 4, 2003, pp. 395-408.

[12] L. Jia, C. Tsui, O. C. Au, K. Jia, "A new rate-complexity-distortion model for fast motion estimation in HEVC", IEEE Transactions on Multimedia, 2018.

[13] Z. Pan, Y. Zhang, S. Kwong, "Efficient motion and disparity estimation optimization for low complexity multiview video coding", IEEE Transactions on Broadcasting, Vol. 61, No. 2, 2015, pp. 166-176.

[14] M. Drulea, S. Nedevschi, "Motion estimation using the correlation transform", IEEE Transactions on Image Processing, Vol. 22, No. 8, 2013, pp. 3260-3270.

[15] H. Yin, H. Jia, H. Qi, X. Ji, X. Xie, W. Gao, "A hardware-efficient multi-resolution block matching algorithm and its VLSI architecture for high definition MPEG-like video encoders", IEEE Transactions on Circuits and Systems for Video Technology, Vol. 20, No. 9, 2010, pp. 1242-1254.

[16] S. Lee, "Fast motion estimation based on adaptive search range adjustment and matching error prediction", IEEE Transactions on Consumer Electronics, 2009.

[17] L. Shen, Z. Liu, T. Yan, Z. Zhang, P. An, "View-adaptive motion estimation and disparity estimation for low complexity multiview video coding", IEEE Transactions on Circuits and Systems for Video Technology, Vol. 20, No. 6, 2010, pp. 925-930.

[18] Y. Huang, J. Ji, K. M. Lee, "Model-based digital image correlation for non-contact deformation measurement of strain field and mechanical property", IEEE Transactions on Industrial Informatics, 2018, pp. 1-9.

[19] W. Feng, Y. Jin, Y. Wei, W. Hou, C. Zhu, "Technique for two-dimensional displacement field determination using a reliability-guided spatial-gradient-based digital image correlation algorithm", Applied Optics, Vol. 57, No. 11, 2018, pp. 2780-2789.

[20] H. Tekwani, K. Raj, "Brightness intensity-based transient motion prediction", Smart Systems: Innovations in Computing. Smart Innovation, Systems and Technologies, Vol. 235, Springer, Jaipur, India, 22-23 January 2021, pp. 1-27.

[21] P. Premaratne, S. Ajaz, M. Premaratne, "Hand gesture tracking and recognition system using Lucas-Kanade algorithms for control of consumer electronics", Neurocomputing, Vol. 116, 2013, pp. 242-249.

[22] J. Weng, P. Cohen, M. Herniou, "Camera calibration with distortion models and accuracy evaluation", IEEE Transactions on Pattern Analysis and Machine Intelligence, Vol. 14 No. 10, 1992, pp. 965-980.

[23] S. Monin, E. Hahamovich, A. Rosenthal, "Single-pixel imaging of dynamic objects using multi-frame motion estimation", Scientific Reports, 2021.

[24] H. Tekwani, K. Raj, "Role of pattern characteristics in cross correlation based motion estimation", Indian Journal of Science and Technology, Vol. 14, No. 41, 2021, pp. 3114-3125.

[25] P. Reu, "Stereo-rig design: lens selection part-3", Experimental Techniques, Vol. 37, No. 1, 2013, pp. 1-3.

[26] Y. Gao, T. Cheng, Y. Su, X. Xu, Y. Zhang, Q. Zhang, "High-efficiency and high-accuracy digital image correlation for three-dimensional measurement", Optics Lasers Engineering, Vol. 65, 2015, pp. 73-80.

[27] M. A. Sutton, J. J. Orteu, H. W. Schreier, "Image correlation for shape, motion and deformation measurements", Springer, Berlin, 2009.

[28] W. LePage, „A practical guide to digital image correlation“, https://digitalimagecorrelation.org/, 2017.

[29] H. Tekwani, K. Raj, "Study of template compression in image correlation based motion estimation", International Journal of Electrical Engineering and Technology, Vol. 12, No. 6, 2021, pp. 308-319.

[30] E. M. C. Jones, M. A. Iadicola, "A good practices guide for digital image correlation", International Digital Image Correlation Society, 2018.

[31] H. Tekwani, K. Raj, "Non-contact motion estimation using image correlation", Proceedings of the IEEE International Conference on Signal Processing and Integrated Networks, Noida, India, 27-28 February 2020, pp. 122-125.

[32] P. Reu, "Stereo-rig design: camera selection part-2", Experimental Techniques, Vol. 36, No. 6, 2012, pp. 3-4.